

## THROMBOSIS AND HEMOSTASIS

## Cardiolipin-mediated procoagulant activity of mitochondria contributes to traumatic brain injury–associated coagulopathy in mice

Zilong Zhao,<sup>1,2</sup> Min Wang,<sup>3</sup> Ye Tian,<sup>1</sup> Tristan Hilton,<sup>2</sup> Breia Salsbery,<sup>2</sup> Eric Z. Zhou,<sup>2</sup> Xiaoping Wu,<sup>2</sup> Perumal Thiagarajan,<sup>4,5</sup> Eric Boilard,<sup>6</sup> Min Li,<sup>3</sup> Jianning Zhang,<sup>1</sup> and Jing-fei Dong<sup>2,7</sup>

<sup>1</sup>Department of Neurosurgery, Tianjin Institute of Neurology, Tianjin Medical University General Hospital, Tianjin, China; <sup>2</sup>BloodWorks Northwest Research Institute, Seattle, WA; <sup>3</sup>Institute of Pathology, School of Basic Medical Sciences, Lanzhou University, Lanzhou, China; <sup>4</sup>Department of Pathology and <sup>5</sup>Department of Medicine, Baylor College of Medicine, Houston, TX; <sup>6</sup>Centre de Recherche du Centre Hospitalier Universitaire de Québec, Department of Infectious Diseases and Immunity, Université Laval and Faculté de Médecine de l'Université Laval, Quebec City, QC, Canada; and <sup>7</sup>Division of Hematology, Department of Medicine, University of Washington School of Medicine, Seattle, WA

## Key Points

- Mitochondria were released from traumatically injured brain into systemic circulation and exposed CL on their surface.
- CL-exposed mitochondria are highly procoagulant and induced traumatic brain injury–associated coagulopathy.

**Cardiolipin (CL) is an anionic phospholipid located exclusively in the mitochondrial inner membrane. Its presence in blood indicates mitochondrial damage and release from injured cells. Here, we report the detection of CL-exposed brain-derived mitochondrial microparticles (mtMPs) at  $17\,547 \pm 2677/\mu\text{L}$  in the peripheral blood of mice subjected to fluid percussion injury to the brain. These mtMPs accounted for  $55.2\% \pm 12.6\%$  of all plasma annexin V-binding microparticles found in the acute phase of injury. They were also released from cultured neuronal and glial cells undergoing apoptosis. The mtMPs synergized with platelets to facilitate vascular leakage by disrupting the endothelial barrier. The disrupted endothelial barrier allowed the release of mtMPs into the systemic circulation to promote coagulation in both traumatically injured and mtMP- or CL-injected mice, leading to enhanced fibrinolysis, vascular fibrin deposition, and thrombosis. This mtMP-induced coagulation was mediated by CL transported from the inner to the outer mitochondrial membrane and was blocked by the scavenging molecule lactadherin. The mtMP-bound CL was  $\sim 1600$  times as active as purified CL in promoting coagulation. This study uncovered a novel procoagulant activity of CL and CL-exposed mitochondria that may contribute to traumatic brain injury–associated coagulopathy and identified potential pathways to block this activity. (*Blood*. 2016;127(22):2763-2772)**

## Introduction

The inability of blood to clot (coagulopathy) is common in patients with traumatic brain injuries (TBIs).<sup>1-3</sup> This TBI-associated coagulopathy is consistently associated with poor clinical outcomes.<sup>3-7</sup> In a report on 3114 patients, the overall hospital mortality rate for isolated TBI with coagulopathy was 50.4% compared with 17.3% for patients without coagulopathy, with an adjusted odds ratio of 2.97.<sup>8</sup> Coagulopathy also promotes delayed cerebral injury secondary to TBI.<sup>6,7</sup>

TBI-associated coagulation abnormalities defined by a number of laboratory tests are found in 10% to 97.2% of patients.<sup>9</sup> This significant disparity is primarily a result of the heterogeneity of patients, the laboratory tests used to define the abnormalities, and the timing of the tests.<sup>4,5,10</sup> Among the common laboratory measurements for coagulation, the elevated levels of D-dimer and fibrin degradation products can be detected within minutes of TBI. These changes are followed by a progressive depletion of fibrinogen.<sup>1,9</sup> Prolonged prothrombin and partial thromboplastin times usually occur at a late stage, indicating a transition from a hyper- to a hypocoagulable state similar to disseminated intravascular coagulation. This phenotype is also evidenced by the presence of pulmonary and cerebral microvascular fibrin deposition and thrombosis in TBI rats.<sup>11,12</sup>

We have recently shown that mouse brains subjected to fluid percussion injury (FPI) produce cellular microparticles that synergize with platelets to disrupt the blood–brain barrier and cause their release into systemic circulation.<sup>12</sup> These brain-derived microparticles (BDMPs) express abundant quantities of surface-exposed and procoagulant phospholipids and tissue factor that are highly enriched in cerebral tissue.<sup>13</sup> The sudden release of a large quantity of procoagulant BDMPs results in systemic and consumptive coagulation that is characterized by a progressive reduction in fibrinogen in the circulation and widespread fibrin deposition in the vasculature of multiple organs.

While studying the production of anti-brain antibodies after TBI, we identified cardiolipin (CL) as a major antigen. Because CL is expressed exclusively in the inner membranes of mitochondria, we hypothesized that mitochondrial microparticles (mtMPs) are released from injured brains into systemic circulation during acute TBI; that these mtMPs promote systemic coagulation, primarily through surface-exposed CL; and that the mtMP-induced procoagulant activity detected in the laboratory contributes to the coagulation abnormalities in mouse models of TBI. Here, we present experimental results that validated these hypotheses and identified a novel activity of CL and CL-exposed

Submitted December 22, 2015; accepted March 13, 2016. Prepublished online as *Blood* First Edition paper, March 21, 2016; DOI 10.1182/blood-2015-12-688838.

The online version of this article contains a data supplement.

The publication costs of this article were defrayed in part by page charge payment. Therefore, and solely to indicate this fact, this article is hereby marked "advertisement" in accordance with 18 USC section 1734.

© 2016 by The American Society of Hematology

mitochondria in regulating coagulation and disrupting the blood–brain barrier.

## Materials and methods

### Mouse models

Blood samples were collected at multiple points after mice were subjected to FPI ( $1.9 \pm 0.1$  atm) to measure the dynamic state of coagulation (supplemental Methods, available on the *Blood* Web site)<sup>12,14,15</sup> and the production of BDMPs and anti-brain antibodies. To test the procoagulant activity of CL and mtMPs without the confounding influence of brain trauma, uninjured C57BL/6J mice (12–16 weeks and 22–25 g; The Jackson Laboratory, Bar Harbor, ME) were injected through the tail vein with bovine heart CL (Avanti Polar Lipids, Alabaster, AL), mouse mtMPs, or phosphate-buffered saline (PBS; pH 7.4). Blood samples were collected 30 minutes after the injection to measure the rates of coagulation and fibrinolysis (D-dimer). The lungs were dissected and processed for the histological evaluation of fibrin deposition in the interstitial vasculature, a hallmark of consumptive coagulopathy. This study was approved by the Institutional Animal Care and Use Committee of BloodWorks Northwest Research Institute.

### Detection and purification of anti-brain antibody

Mouse brain homogenates (MBHs) were generated (supplemental Methods) and used to coat microtiter plates (20  $\mu\text{g}/\text{mL}$ ) overnight at 4°C. The plates were blocked with 1% bovine serum albumin for 2 hours at 4°C and washed with PBS containing 0.05% Tween 20. They were then incubated with cell-free plasma from FPI and sham mice (1000–60 000 dilutions) for 2 hours at room temperature (RT), followed by horseradish peroxidase–conjugated goat anti-mouse IgG (Southern Biotechnology Associates Inc., Birmingham, AL) for 1 hour at RT. The bound antibody was detected with the horseradish peroxidase substrate 3,3',5,5'-tetramethylbenzidine at OD450 nm. IgGs and anti-CL antibody were purified from the plasma of FPI mice, using a Crosslink Magnetic IP/Co-IP kit (Thermo Fisher Scientific, Waltham, MA) and CL-coupled beads, respectively, and tested for their binding to MBH, mtMPs, and CL (supplemental Methods).

### Flow cytometry

For flow cytometric analyses, mtMPs were defined as microparticles identified first by their size ( $<1 \mu\text{m}$ ), as calibrated by 0.5-, 0.9-, and 3- $\mu\text{m}$  standard microbeads (Biotec, Marseille, France), and then by their labeling with the mitochondria-specific fluorescent dye MitoTracker Green (Thermo Fisher Scientific), a membrane-potential-independent green fluorescent dye that stains mitochondria in live cells.<sup>16</sup> Blood samples collected from FPI and sham mice (0.38% sodium citrate anticoagulated) were diluted 50% with PBS, incubated with MitoTracker Green (100 nM) for 30 minutes at RT, and analyzed on an LSR II flow cytometer (Beckon Dickinson, San Jose, CA). Sphero Accucount Ultra-rainbow Fluorescent Particles (Spherotech, Lake Forest, IL) were used to count the number of microparticles. For data validation, mtMPs were also stained with 1  $\mu\text{M}$  10-Nonyl acridine orange (Thermo Fisher Scientific; 30 minutes at RT), a membrane-permeable fluorescent dye that specifically binds CL.<sup>17</sup> All buffers used in flow cytometry were filtered with a 0.1- $\mu\text{m}$  filter (EDM Millipore, Billerica, MA) to reduce particle contamination.

Neuronal microparticles were recognized for their expression of neuron-specific enolase (NSE), detected by a monoclonal antibody (Abcam, Cambridge, MA), and phosphatidylserine (PS) labeled with allophycocyanin-conjugated human recombinant annexin V (eBioscience, Inc., San Diego, CA) and MitoTracker Green. The specificity of annexin V binding was verified with 5 mM EDTA, which chelates calcium to block the binding. Flow cytometry was also used to detect annexin V binding to CL coupled to latex microspheres (supplemental Methods).

### Injury-induced production of mtMPs in vitro

Human neuroblastoma SH-SY5Y and glioblastoma T98G cells (both from American Type Culture Collection, Manassas, VA) were tested as surrogates for

neurons and glial cells, respectively. They were cultured at 37°C with 5% CO<sub>2</sub> at equal seeding densities in the complete Dulbecco's modified Eagle's medium (Corning, Tewksbury, MA) containing 10% fetal bovine serum. After 5 days in culture, the cells were washed with PBS and stimulated with either 10  $\mu\text{g}/\text{mL}$  calcium ionophore A23187 (Fisher Bioreagents, Waltham, MA) or 2  $\mu\text{g}/\text{mL}$  lipopolysaccharides (LPS; Sigma-Aldrich, St. Louis, MO) for 30 minutes at 37°C. A23187 and LPS served as surrogates for apoptotic and inflammatory insults, respectively. The culture media from the stimulated and unstimulated cells were collected and centrifuged at 16 000g for 10 minutes to collect the supernatant, where mtMPs labeled with MitoTracker Green were detected with flow cytometry.

### Purification of mtMPs

mtMPs were purified by 3 methods to cross-validate the results. First, they were isolated from the plasma of FPI mice with an anti-TOM22 antibody, using a commercial kit (Miltenyi Biotec, Auburn, CA; supplemental Methods). Second, they were purified with a commercial Qproteome mitochondria isolation kit (Qiagen, Valencia, CA), which isolated mitochondria by dense gradient centrifugation. Finally, mtMPs labeled with MitoTracker Green were collected through fluorescence-activated cell sorting (FACS Aria, Beckon Dickinson). mtMPs purified through these methods were verified with 10-Nonyl acridine orange labeling. The isolated mtMPs were collected by centrifugation at 100 000g for 1 h at 4°C and resuspended in PBS at appropriate densities for testing.

### Isolation and quantification of mitochondrial DNA

Mitochondrial DNA (mtDNA) was extracted from cell-free plasma of both FPI and sham mice and from cell culture supernatant, using a QIAamp DNA Micro Kit (Qiagen). It was amplified with quantitative polymerase chain reaction<sup>18</sup> with primers and probes (supplemental Table 1), using the Rotor-Gene PCR kit (Qiagen) through 40 cycles of 95°C for 3 seconds and 60°C for 10 seconds after initial DNA denaturing at 95°C for 3 minutes. These primers and probes are specific for detecting mouse and human mtDNA in plasma samples from TBI mice and human neuronal and glial cells in culture, respectively. The quantitative polymerase chain reaction standards were mtDNA from mouse brain and human glial cells at known concentrations of 0.008, 0.04, 0.2, 1, and 5 ng/ $\mu\text{L}$ .

### Assay for endothelial cell barrier function

Human umbilical vein endothelial cells (HUVECs; Lonza) were grown to confluence in the endothelial growth basal medium-2 (Lonza) and stimulated with CL or isolated mtMPs for 2 hours at 37°C. The cells were washed with PBS, fixed by 4% formaldehyde, and permeabilized by 0.1% Triton X-100 in PBS for 30 minutes each at RT. They were then blocked with 1.5% bovine serum albumin for 30 minutes and stained with a mouse anti-CD31 antibody (Abcam, Cambridge, MA) and a rabbit anti-von Willebrand factor (VWF) antibody (Dako North America, Carpinteria, CA) for 1 hour at RT. The control cells were stained with isotype control IgGs. After washing, the cells were stained with Alexa Fluor 594-conjugated goat anti-rabbit (Thermo Fisher Scientific) and Alexa Fluor 488-conjugated goat anti-mouse (Thermo Fisher Scientific) antibodies for 60 minutes at RT and then counterstained with 4',6-diamidino-2-phenylindole (Sigma-Aldrich, St Louis, MO). The conditioned media from the cells stimulated with CL, mtMPs, or PBS were centrifuged at 1500g for 20 minutes to remove cells, and were then probed for VWF as a marker for endothelial cell activation using ELISA (Ramco Laboratories, Inc., Stafford, TX; supplemental Methods).

In addition, HUVECs were grown on a collagen-coated polyethylene terephthalate membrane (1  $\mu\text{m}$  pore) in a transwell (EDM Millipore, Billerica, MA) until they were more than 95% confluent.<sup>12</sup> They were stimulated with CL or mtMPs in the presence and absence of fresh platelets (300 000/ $\mu\text{L}$ ) for 3 hours at 37°C. After washing, the HUVECs were incubated with 70 kDa fluorescein isothiocyanate (FITC)-Dextran (EDM Millipore, Billerica, MA) for 30 minutes at 37°C. The culture media in the bottom chambers were collected to measure FITC-Dextran fluorescence at 485 nm excitation and 535 nm emission.

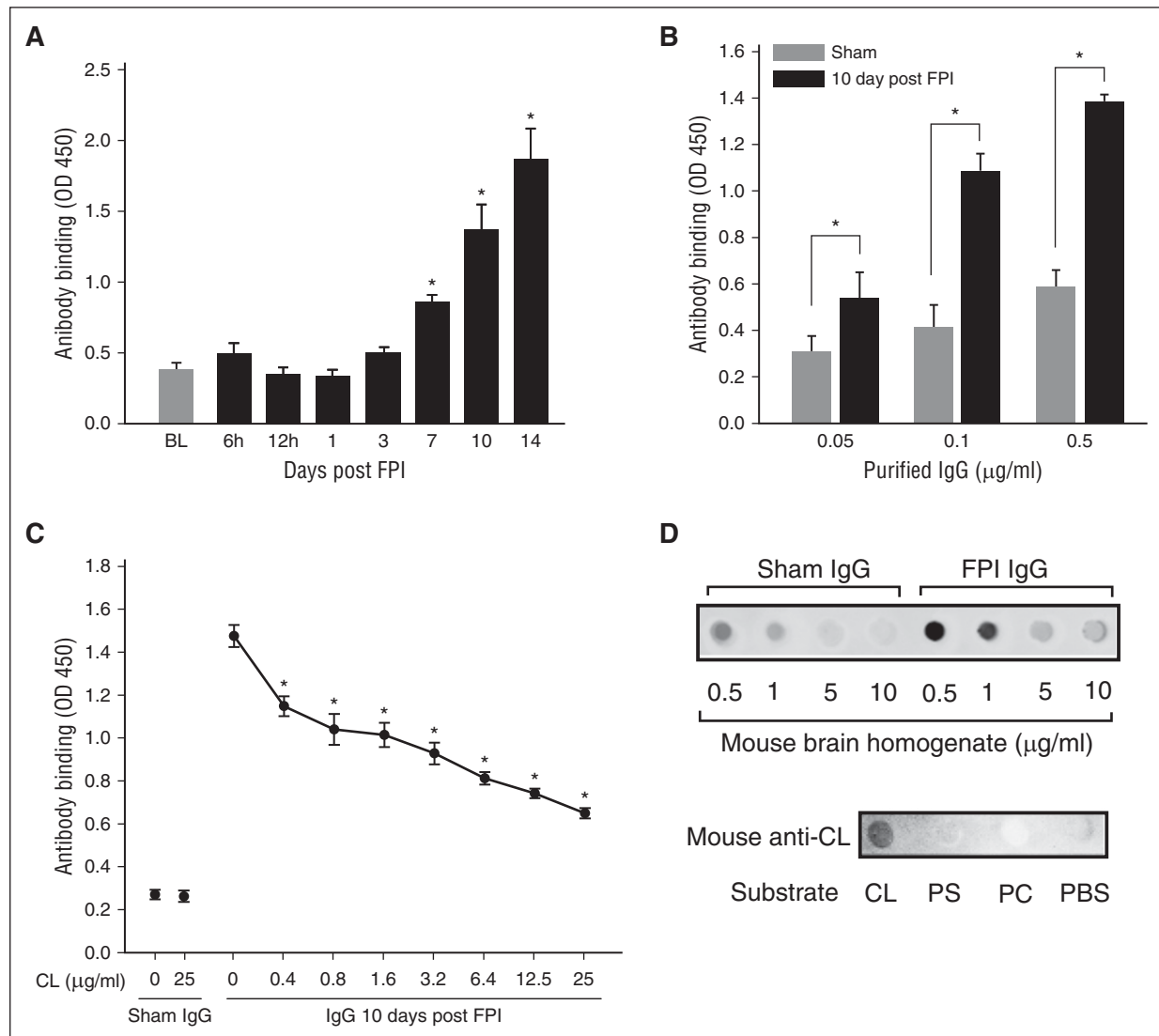


**Figure 1. Antibrain and anti-CL antibodies were detected in FPI mice.** (A) Immunoreactivity to MBH of 1/1000 diluted plasma from FPI mice at different postinjury times ( $n = 6$ /point; repeated measures ANOVA,  $*P < .01$  vs baseline before FPI). (B) Binding of IgGs purified from sham or FPI mice to MBH ( $n = 6$ /dose; paired Student  $t$  test,  $*P < .01$ ). (C) Anti-brain IgGs (0.5  $\mu\text{g}/\text{mL}$ ) from FPI mice were incubated with increasing concentrations of CL for 30 minutes, and then with MBH for 30 minutes at RT ( $n = 5$ -7/dose; repeated measures ANOVA,  $*P < .01$  vs IgG at 0 CL). (D, top) CL blotted to nitrocellulose membrane was probed with IgGs (0.25  $\mu\text{g}/\text{mL}$ ) from sham and FPI mice (10 days post-FPI) in the presence of increasing amounts of MBH. (Bottom) Phosphatidylcholine (PC), PS, and CL blotted onto nitrocellulose membrane (18  $\mu\text{g}/\text{spot}$ ) were probed with the CL antibody purified from plasma collected 10-14 days after FPI from TBI mice.

## Electron microscopy

CL micelles (supplemental Methods) were suspended in PBS (pH 7.4) to a final concentration of 40  $\mu\text{g}/\text{mL}$  and immobilized onto Formove-coated slides by air-drying. The slides were sputter-coated with platinum and examined under a scan electron microscope (JEM-1230 SEM by JEOL, Tokyo, Japan).

Freshly purified plasma microparticles from FPI mice and brain sections were fixed in 2.5% glutaraldehyde for 24 hours at 4°C, washed with a 0.1-M cacodylate buffer, and fixed again in 2% aqueous OsO<sub>4</sub>/0.2 M cacodylate for 2 hours at 4°C. They were dehydrated and embedded in Epon 812 for 2 hours. Ultrathin sections were made and sequentially treated with uranyl acetate for 2 hours and lead citrate for 5 minutes before being heat-dried and observed through transmission electron microscopy (JEM-1400 by JEOL, Tokyo, Japan).

## Statistical analysis

Categorical (frequency) variables were expressed as percentages and continuous variables as the mean  $\pm$  SEM. The data were analyzed using Sigma plot (V. 11.2) for paired Student  $t$  test or 1-way or repeated

measures ANOVA, as specified in each analysis. A value of  $P \leq .05$  was considered statistically significant.

## Results

### FPI-induced anti-brain antibodies cross-reacted with CL

Antibodies in the plasma collected from mice 10 and 14 days after FPI interacted with MBHs (Figure 1A), with a maximal titer of 16 000. This result was validated by the binding of IgGs purified from the plasma of FPI mice to MBHs (Figure 1B). The binding was dose-dependently blocked by free CL with a maximal inhibition of  $39.3\% \pm 13.8\%$  achieved at 25  $\mu\text{g}/\text{mL}$  CL (Figure 1C). In reciprocal experiments, the binding of IgG from FPI mice to CL was dose-dependently blocked by MBHs (Figure 1D, top). Anti-CL antibody purified from plasma of FPI mice bound CL, but not PS or PC (Figure 1D, bottom). The detection of

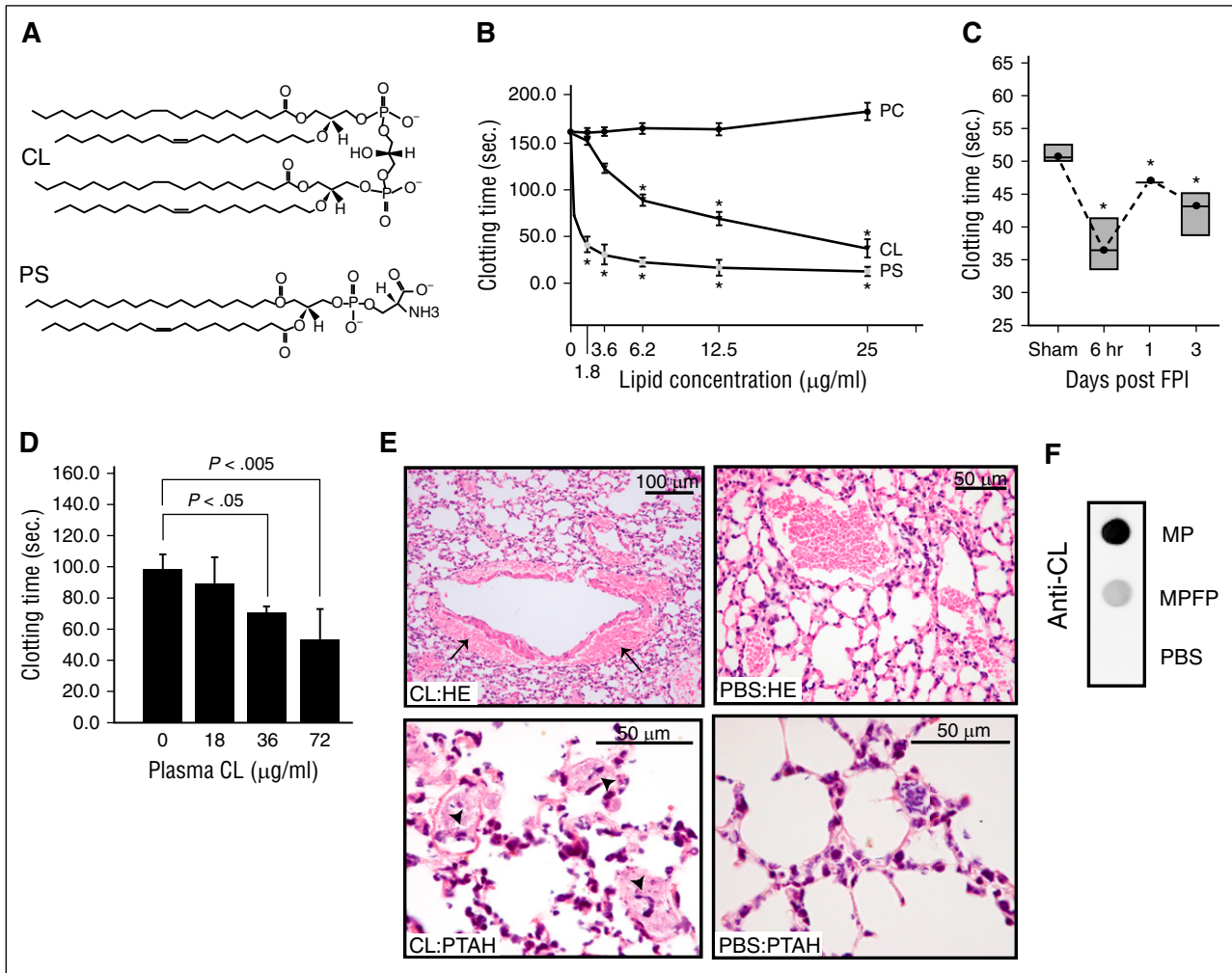


**Figure 2. CL was procoagulant and microparticle-bound.** (A) A structural comparison between CL and PS. (B) The time to clot of phospholipid-depleted plasma in the presence of purified CL, PS, or PC ( $n = 6$ ; 1-way ANOVA,  $*P < .01$  vs PC). (C) Clotting times of plasma collected at different points from C57BL/6J mice subjected to FPI or sham surgery ( $n = 6$ ; 1-way ANOVA,  $*P < .01$  vs sham mice). (D) Clotting time of plasma collected from non-injured C57BL/6J mice 30 minutes after CL injection ( $n = 6$ /group; 1-way ANOVA,  $*P < .05$  vs sham mice). (E) Hematoxylin and eosin (HE, top) and phosphotungstic acid-haematoxylin (PTAH, bottom) stains of the lungs show perivascular accumulation of erythrocytes resulted from vascular leakage (top left) and intravascular fibrin deposition (arrow, bottom left) in mice injected with CL, but not those injected with PBS (right panels, 5–10 evaluations/treatment). (F) Anti-CL antibody detected CL in microparticles, not microparticle-free plasma (MPFP) collected from mice 6 hours after FPI (MPFP was prepared as previously described<sup>12</sup>).

high-titer anti-CL antibody indicated the substantial release of CL during the acute phase of FPI, which led us to study the effects of CL and its cellular carriers on coagulation in the first 24 hours after FPI. The biological activity of the anti-brain antibodies, including anti-CL antibody, is therefore not described here.

### CL was procoagulant and microparticle-bound

CL [1,3-bis(sn-3'-phosphatidyl)-sn-glycerol] is an anionic phospholipid that contains 2 phosphatidic acid moieties connected to a glycerol backbone to form a dimer with 4 alkyl groups and 2 potential negative charges.<sup>19</sup> This structure is homologous to the procoagulant PS (Figure 2A), but it is not known whether CL promotes coagulation. Here, we show that freshly prepared CL micelles induced clot formation in phospholipid-depleted plasma in a dose-dependent manner (Figure 2B). This procoagulant activity reached a maximum at 25 μg/mL, a level comparable to an equal concentration of PS. Consistent with our recent report,<sup>12</sup> mice subjected to FPI rapidly developed a procoagulant state, defined by a shortened clotting time (Figure 2C) and increased thrombin generation (Table 1). This hypercoagulable state was similarly induced through

the injection of the carrier-free CL into uninjured mice (Figure 2D). The CL-injected mice presented extensive fibrin deposition in the pulmonary interstitial microvasculature and vascular leakage, but the PBS-injected mice did not. The vascular leakage resulted in bleeding, as evidenced by the accumulation of erythrocytes in the perivascular space (Figure 2E).

As an anionic phospholipid with hydrophobic tails,<sup>19</sup> CL is expected to be in a micellar, lamellar, or hexagonal state. CL micelles were indeed detected in solution at 40 μg/mL by scan electron microscopy (supplemental Figure 1). However, we found that CL was detected in the microparticle-containing, but not the microparticle-free,

**Table 1. Thrombin generation induced by plasma from FPI mice**

	Days post-FPI				P value*
	Sham	0.25	1	3	
Lag time, minute	4.87	5.21	4.46	4.74	.781
Area under the curve, nM × minute	46.06	59	65.06	53.9	.107
Peak production, nM	5.18	6.38	9.44	6.57	.036

\*Analyzed by 1-way ANOVA.



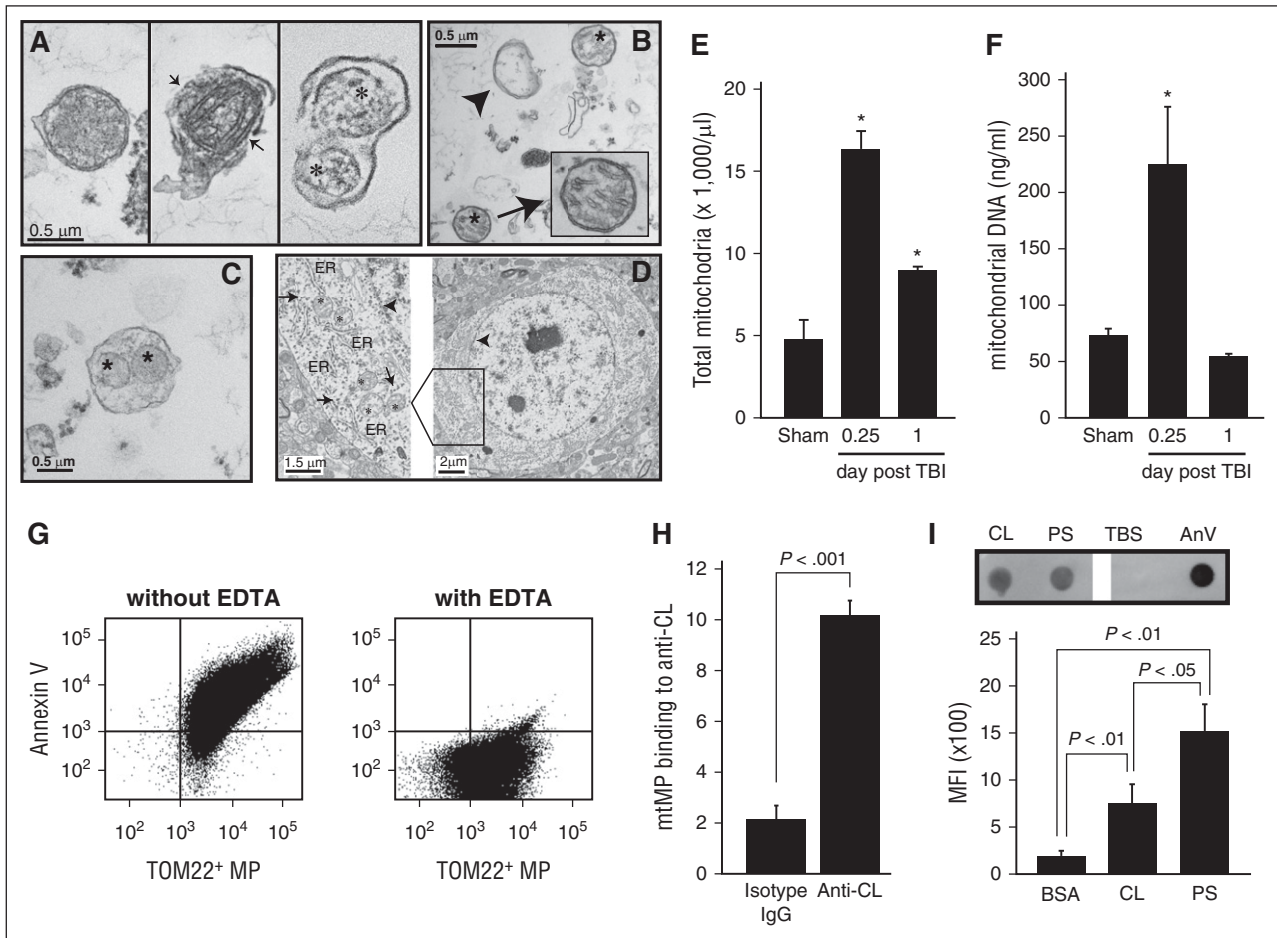


**Figure 3. mtMPs were detected in plasma from FPI mice and contained surface-exposed CL.** Transmission electron microscope images. (A) Intact (left) and membrane-disrupted (middle, arrow) mitochondria and mitochondria-embedded BDMP (right; asterisk, mitochondria) detected in plasma of FPI mice. (B) Mitochondria (asterisk), membrane microparticles (arrowhead), and (C) mitochondria-embedded membrane microparticles (\*) from purified BDMPs. (D) A section of an uninjured mouse brain shows a dense perinuclear distribution of mitochondria (left, arrowhead: nuclear membrane). A locally enlarged image further shows mitochondria (asterisk) and endoplasmic reticulum (ER) and membrane-bound/free polyribosomes (arrow). (E) Total mtMPs and (F) mtDNA detected in plasma samples from sham and FPI mice. (G) Annexin V bound to more than 80% of mtMPs purified by TOM22 antibody (left), and the binding was abolished by EDTA (right). (H) Anti-CL antibody purified from FPI mice, but not a control IgG, bound purified mtMPs. (I, top) CL and PS captured to the nitrocellulose membrane were incubated with human annexin V (PBS and annexin V as controls). Annexin V bound to the phospholipids was detected by a polyclonal annexin V antibody. (Bottom) Allophycocyanin-conjugated annexin V bound to CL and PS coated on microbeads detected by flow cytometry ( $n = 3$ -6/group; paired Student  $t$  test).

fraction of the plasma from FPI mice (Figure 2F), consistent with our report that cellular microparticles, not microparticle-free plasma promote the phospholipid-dependent coagulation.<sup>12</sup>

#### mtMPs were released in the acute phase of TBI and were procoagulant

CL is located exclusively in the mitochondrial inner membrane and constitutes ~20% of the total mitochondrial lipids.<sup>20,21</sup> Figures 1 and 2 therefore indicate that a substantial number of mtMPs were released during acute FPI and that CL was exposed on those mtMPs. Isolated and plasma membrane-embedded mitochondria, measuring 0.3-0.6  $\mu\text{m}$  in diameter, were indeed detected in plasma from mice 6 hours after FPI and in purified BDMPs by transmission electron microscopy (Figure 3A-C) and flow cytometry (Figure 3E). These mtMPs had intact (Figure 3A, left) or partially broken (Figure 3A, middle) membranes. The plasma membrane that embedded mitochondria was also found to be broken in some microparticles from TBI mice (Figure 3A, right). The mitochondria-embedded microparticles expressed the neuronal marker NSE (supplemental Figure 2), suggesting they came from

injured brains. Consistent with these data, mtDNA was amplified in plasma from FPI mice 6 hours after injury (Figure 3F). Quantitatively,  $17\,547 \pm 2677$  mtMPs/ $\mu\text{L}$  were detected in mouse plasma samples collected 6 hours after FPI. These mtMPs accounted for  $55.2\% \pm 12.6\%$  of the annexin V-binding microparticles found during acute injury. This level is significantly higher than those in samples collected on postinjury days 3 ( $33.3\% \pm 6.9\%$ ), 7 ( $29.6\% \pm 5.1\%$ ), and 14 ( $28.8\% \pm 8.6\%$ ;  $n = 3$ -7/group; repeated measures ANOVA,  $P < .05$ ). Consistent with this predominant release of mtMPs, brain sections of uninjured mice showed a high density of mitochondria in the perinuclear region (Figure 3D). Together, these data indicate that mtMPs constitute a major type of microparticles released from acutely injured brains.

To test the procoagulant activity of mtMPs without the confounding influence of trauma, we purified mtMPs using gradient centrifugation. The identity of these mtMPs was validated by their being labeled with the fluorescent dye 10-Nonyl acridine orange (supplemental Figure 3), which specifically binds CL.<sup>17</sup> Strikingly, more than 80% of mtMPs bound annexin V (Figure 3G). This high rate of annexin V binding was also detected in mtMPs purified from FPI mouse plasma by the TOM22

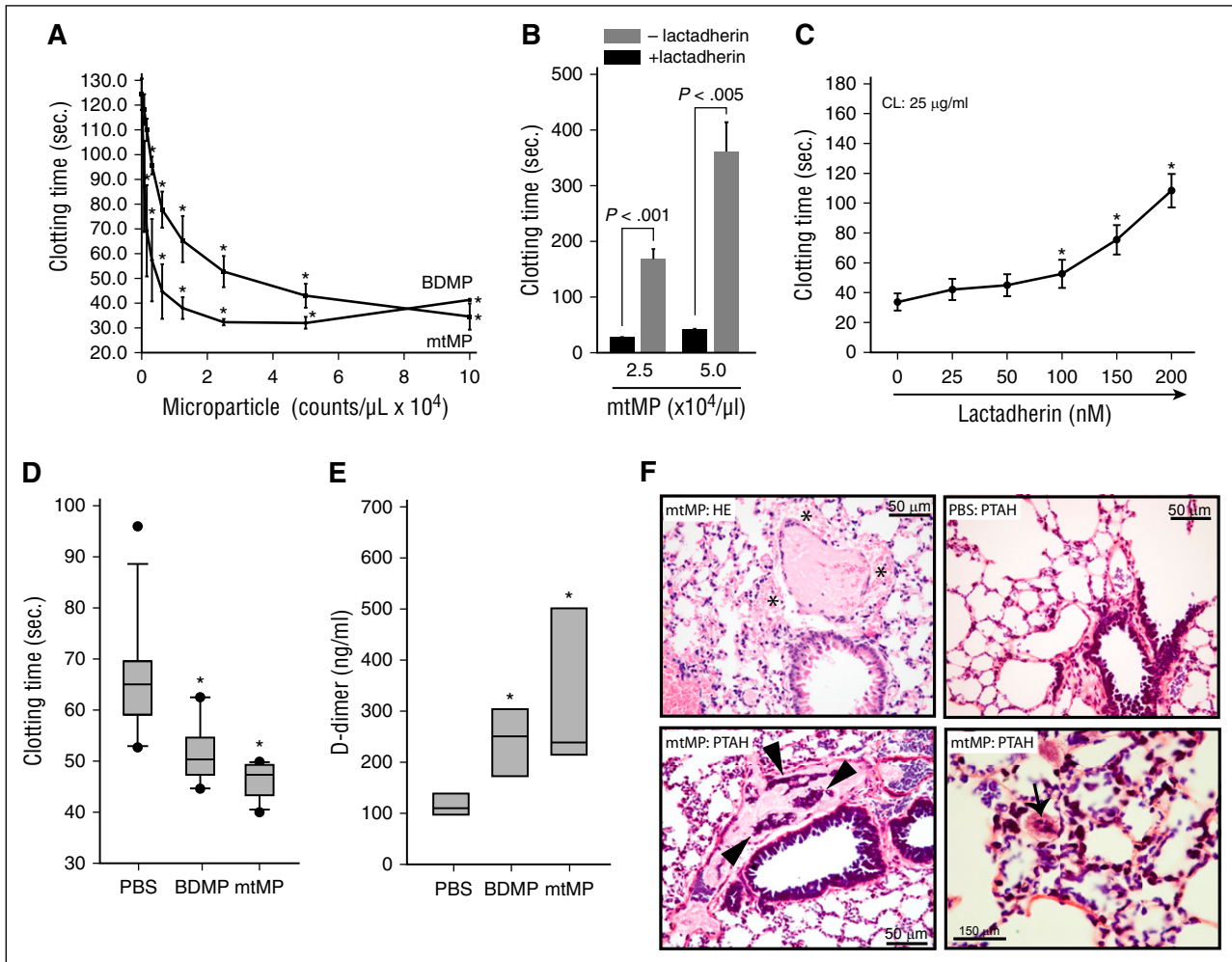


**Figure 4. mtMPs were procoagulant.** (A) A dose-dependent acceleration of plasma clotting time induced by mtMPs and BDMPs ( $n = 3$ /point; repeated measures ANOVA,  $*P < .001$  vs no microparticles). (B) This mtMP-induced coagulation was blocked by 200 nM lactadherin ( $n = 3$ /group; paired  $t$  test). (C) Plasma clotting induced by 25  $\mu\text{g}/\text{mL}$  CL in the presence of increasing concentrations of lactadherin ( $n = 3$ ; repeated measures ANOVA,  $*P < .01$  vs no CL). Uninjured mice were injected with PBS, mtMPs, or BDMPs (both at  $2.5 \times 10^4/\mu\text{L}$ ). Plasma samples were collected 30 minutes after injection to measure clotting time (D;  $n = 6$ /group; repeated measures ANOVA,  $*P < .01$  vs PBS) and D-dimer (E;  $n = 6$ /group; repeated measures ANOVA,  $P < .01$  vs PBS). (F) HE stain of the lungs from mtMP-injected mice shows erythrocyte accumulation in the extravascular space (\*, top left) compared with PBS-injected mice (top right), and extensive fibrin deposition in the dilated pulmonary interstitial vessels (arrowheads, bottom left) compared with PBS-injected mice (top right). Microvascular fibrin-rich thrombosis is shown in the pulmonary vasculature (arrow, bottom right) of mtMP-injected mice. Images are representative of 6 mice/group.

antibody or by flow cytometric cell sorting (supplemental Figure 4), suggesting the annexin V binding is an intrinsic characteristic of mitochondria released from injured brains. Because mitochondria lacks de novo synthesis of PS,<sup>22,23</sup> and PS transported from the endoplasmic reticulum to the mitochondria<sup>24-26</sup> is rapidly converted to phosphatidylethanolamine (PE) by PS decarboxylase located in the inner membrane,<sup>24</sup> we hypothesize that annexin V binds CL that has been transported from the inner to the outer membrane of mitochondria. This hypothesis is supported by the findings that anti-CL antibody bound nonpermeabilized mtMPs (Figure 3H) and annexin V bound purified CL (Figure 3I)

The surface exposure of procoagulant CL suggests that mtMPs promote coagulation. Here, we show that purified mtMPs dose-dependently promoted clot formation in vitro at a level similar to that of BDMPs (Figure 4A). Lactadherin (milk fat globule-EGF factor 8), a PS-binding scavenging molecule involved in the clearance of apoptotic cells,<sup>27</sup> blocked the procoagulant activity of mtMPs (Figure 4B) and CL (Figure 4C). Consistent with these in vitro observations, mtMPs injected into uninjured mice induced a hyper-turn-hypocoagulable state within 30 minutes, characterized by a shortened clotting time

(Figure 4D), an increased level of plasma D-dimer (Figure 4E), and fibrin deposition in the pulmonary vasculature (Figure 4F). mtMP also induced vascular leakage (Figure 4F, top left) similar to that found in CL-injected mice (Figure 2E, top right) and fibrin-rich thrombosis in the pulmonary interstitial vessels (Figure 4F, bottom right). We conclude that this mitochondrial procoagulant activity was mediated by surface-exposed CL on the basis of several lines of evidence: first, PS accounted for only 0.7% of the total mtMP phospholipids measured by mass spectrometry (LC/MS/MS, Avanti Polar Lipids); second, neither PC nor PE, which accounted for 54.6% and 23.8% of the total mitochondrial phospholipids measured by LC/MS/MS, respectively, promoted coagulation (supplemental Figure 5); third, anti-CL antibody from FPI mice bound nonpermeabilized mtMP (Figure 3H); fourth, annexin V bound directly to CL (Figure 3I); and fifth, lactadherin blocked the mtMP-induced clotting of phospholipid-depleted plasma (Figure 4B).

We also determined that BDMPs contained 75.8 ng of CL per microgram of proteins by LC/MS/MS (Avanti polar lipids). This measurement allowed us to calculate that  $5 \times 10^4/\mu\text{L}$  microparticles that induced significant procoagulant activity (Figure 4) contained

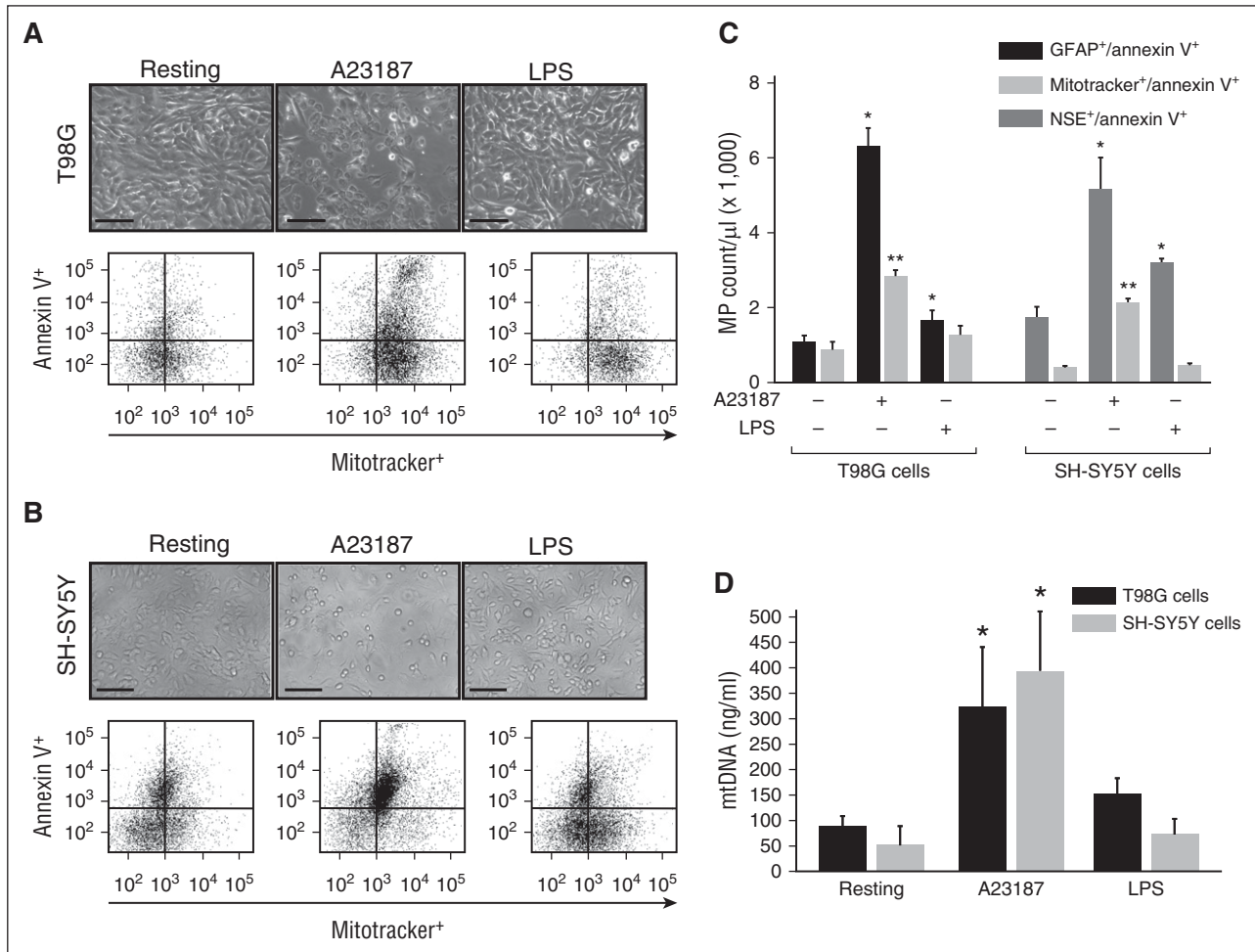


**Figure 5. mtMPs were released from cultured neurons and glial cells.** (A) Human glioblastoma T98G (A) and neuroblastoma SH-SY5Y (B) cells before (left) and after (middle) stimulated with the calcium ionophore A23187 or LPS (right) (bar = 50  $\mu$ m). (A-B, top) Morphological changes; (bottom) levels of mtMPs detected in conditioned media from these cells before and after stimulations. (C) MitoTracker Green<sup>+</sup> glial and neuronal cell microparticles that were annexin V<sup>+</sup> detected by flow cytometry. The relative levels of annexin V<sup>+</sup>/MitoTracker Green<sup>+</sup> T98G cells and SH-SY5Y cells that were also positive for GFAP and NSE, respectively (n = 3-5; 1-way ANOVA, \**P* < .011 and \*\**P* < .005 vs resting cells). (D) Levels of mitochondrial DNA in the supernatants of T98G and SH-SY5Y cells at resting and after stimulation with either A23187 or LPS (n = 3-5; 1-way ANOVA, \**P* < .001 vs resting cells).

~15.2 ng mitochondria-bound CL. This quantity of mtMPs had a procoagulant activity equivalent to that of ~25  $\mu$ g/mL of CL micelles (Figure 2B vs Figure 4A), suggesting that mtMP-bound CL was 1600 times as active as carrier-free CL in promoting coagulation.

#### Neuronal and glial cells released mtMPs after injury

Glial T98G and neuronal SH-SY5Y cells were stimulated with the calcium ionophore A23187 or endotoxin (LPS) to mimic apoptotic or inflammatory insults, respectively. Both T98G (Figure 5A) and SH-SY5Y cells (Figure 5B) underwent rapid shrinkage and some detachments after A23187 treatment, but they remained mostly attached after LPS stimulation. Microparticles were detected in the condition media from cells stimulated with A23187 and, to a lesser degree, those stimulated with LPS (Figure 5C). mtMPs accounted for 46.6% and 42.8% of the total annexin V-binding glial (GFAP<sup>+</sup>) and neuronal (NSE<sup>+</sup>) microparticles, respectively, in A23187-stimulated cells. In contrast, mtMPs were minimally detected in LPS-stimulated neurons and glial cells. mtDNA was also amplified in the supernatant of neuronal and glial cells stimulated with A23187, but minimally with LPS (Figure 5D). These data indicate that cultured neuron and glial cells also produced mitochondria upon apoptotic injury at a level comparable to that found in FPI mice.

#### CL and mtMPs affected endothelial cell integrity

The treatment of cultured HUVECs with either 25  $\mu$ g/mL CL or 2.5  $\times 10^4$   $\mu$ L mtMP reduced the expression of CD31 (PECAM-1; Figure 6A-D), a widely used marker for endothelial cell junction. This finding is consistent with the perivascular accumulation of erythrocytes observed in the lungs of mice injected with CL (Figure 2E) or mtMPs (Figure 4F). The CL or mtMPs also activated endothelial cells to release VWF (Figure 6G). Using a transwell cell migration assay, both CL and mtMPs were found to promote the FITC-Dextran leakage through the endothelial cell barrier in the presence of platelets (Figure 6H). These data demonstrate that CL and mtMPs disrupt the integrity of vascular endothelial cells to promote vascular leakage in a platelet-dependent manner.

## Discussion

We made several observations that together define a novel CL-mediated procoagulant activity of mitochondria that may contribute to the laboratory-defined coagulation abnormalities in mice with acute TBI. First, we demonstrated that the anionic phospholipid CL was a



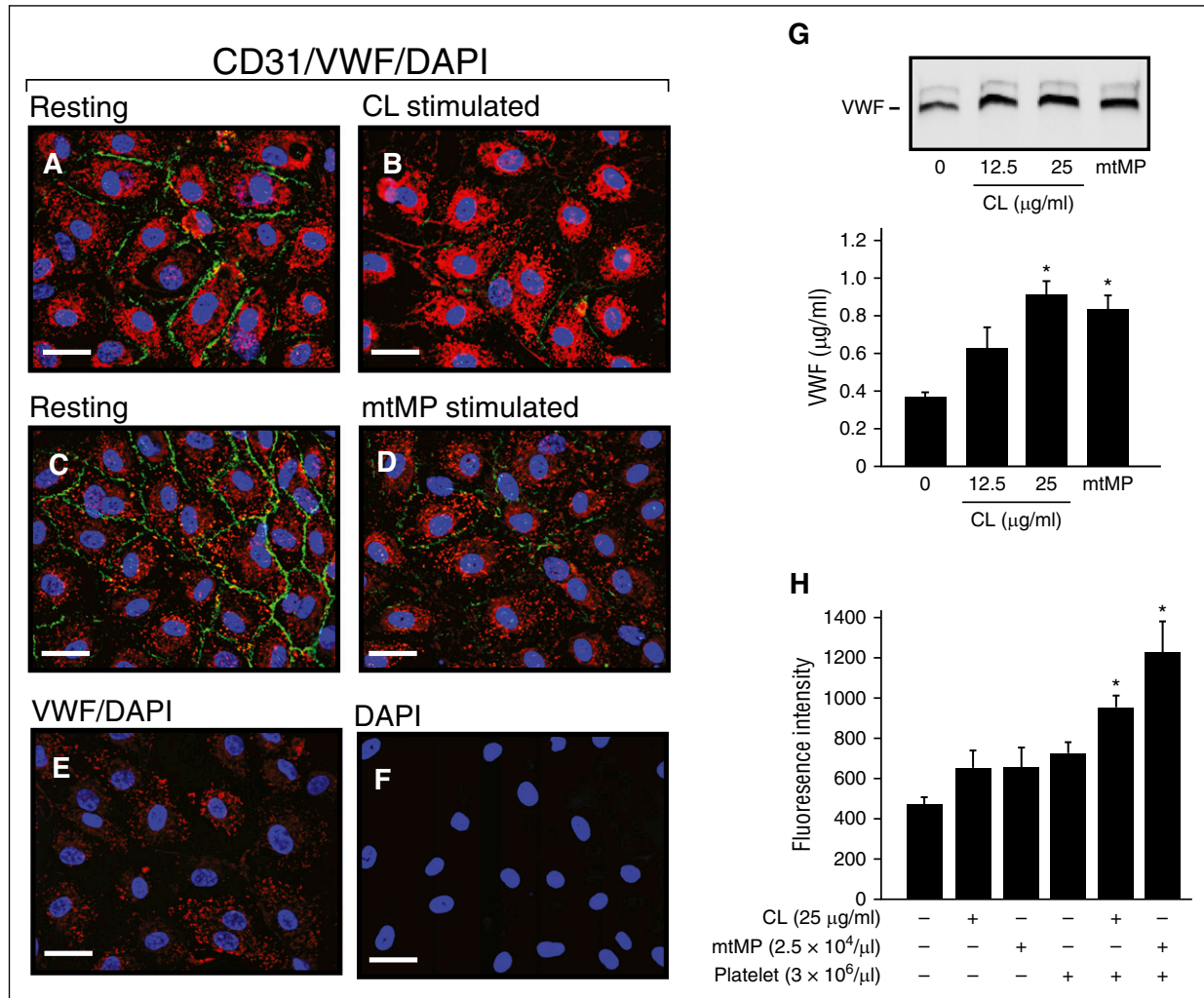


**Figure 6. CL and mtMP activated ECs and disrupted their barrier function.** HUVECs before (A,C) and after stimulation with CL (B, 25 μg/mL) or mtMP (D, 2.5 × 10<sup>4</sup>/μL) for 2 hours at 37°C were stained for CD31 (PECAM1, green), VWF (red), and 4',6-diamidino-2-phenylindole (blue) to mark cell-cell junction, endothelial cells, and the nucleus, respectively. Resting cells stained with VWF (E) and 4',6-diamidino-2-phenylindole (F) served as controls (representative of 3-5 experiments; bar = 20 μm). (G) The conditioned media from cultured ECs before and after treated with CL or mtMPs were analyzed for VWF by immunoblot (top) and ELISA (bottom). (H) Confluent HUVECs on collagen-coated PET membrane were stimulated with CL or mtMPs in the presence and absence of fresh platelets for 3 hours at 37°C, followed by incubation with FITC-Dextran for 30 minutes at 37°C. Fluorescent dextran was detected in the bottom chambers (n = 3-4; 1-way ANOVA).

major antigen for the anti-brain antibodies produced in TBI mice (Figure 1). This CL antibody was specific and did not cross-react with the homologous PS (Figure 1G). This finding is concordant with the presence of peroxidized CL in injured brains,<sup>28,29</sup> and of anti-CL antibody in patients with stroke<sup>30</sup> and TBI.<sup>31</sup> Although the present study was not designed to investigate the effect of anti-CL antibody on coagulation, the predominant presence of anti-CL antibody did lead us to study the effects of CL and its carriers on the development of laboratory-defined coagulopathy in mice subjected to TBI.

Second, the anionic CL promoted coagulation (Figure 2B,D-E), consistent with its ability to bind annexin V (Figure 3I) and structural homology to PS (Figure 2A). This homology may have also allowed lactadherin, which blocks PS-mediated coagulation,<sup>12,32,33</sup> to inhibit CL-mediated coagulation (Figure 4C). We further show that the CL detected in TBI mice was primarily mitochondria-bound (Figure 2G), suggesting a substantial release of mitochondria from acutely injured brains.

Third, mitochondria were released from injured brains (Figure 3A-C; supplemental Figure 2). This is consistent with a previous report that activated platelets release mtMPs.<sup>18,34</sup> Furthermore, mtMPs were detected at a disproportionately high level during acute TBI (Figure 3A-F),

accounting for more than 55% of annexin V<sup>+</sup> microparticles. This acute release of mtMP was further validated by the ability of cultured neurons and glial cells to produce mitochondria-rich microparticles in response to apoptotic stimulation (Figure 5). Although no quantification has been made, as they have been for hepatocyte (~1700 mitochondria/hepatocyte)<sup>35</sup> and platelets (4-5/platelet),<sup>18</sup> brain cells are expected to be mitochondria-rich to meet their high energy needs, as shown by the densely packed mitochondria in brain cells (Figure 3D). Intracellular mitochondrial dysfunction and molecules released from damaged mitochondria (DAMPs) are well documented for their contributions to disease states.<sup>36-40</sup> Our data further suggest that mtMPs possess a unique procoagulant activity that differs from intracellular mitochondrial dysfunctions and DAMPs.

Finally, CL that is located exclusively in the mitochondrial inner membrane of healthy cells<sup>20,21</sup> was transported to the outer membrane when mitochondria were released from injured cells. This conclusion is supported by the following experimental data: anti-CL antibody was predominantly generated in TBI mice and bound nonpermeabilized mitochondria (Figure 1C-D,H), and annexin V, which binds anionic PS,<sup>41-43</sup> bound CL (Figure 3I) and nonpermeabilized mtMPs



(Figure 3G; supplemental Figure 4). The CL externalization has been reported in primary cortical neurons and SH-SY5Y cells after they were treated with rotenone,<sup>44</sup> which disrupts the mitochondrial electron transport chain to induce apoptosis<sup>45</sup> and in the cardiomyocytes of coronary occluded hearts.<sup>44,46</sup>

This mitochondrial procoagulant activity is mediated primarily by exposed CL, rather than PS, because there was only a residual amount of mitochondrial PS because of the lack of de novo synthesis and the rapid conversion of imported PS to PE<sup>22-26</sup> that has no net charge.<sup>47</sup> PC and PE constitute almost 80% of the mitochondrial phospholipids, but did not promote coagulation (supplemental Figure 5). More important, the CL exposed on mtMPs was more than 1600 times as active as CL micelles, probably because a high concentration of CL is needed for micelles to form in the absence of membrane support; the CL expressed on mtMPs is optimally orientated for interactions with coagulation factors; and the procoagulant activity is enhanced by interactions of CL with other (phospho)lipids and protein cofactors, as exemplified in CL's ability to initiate the complement activation by forming a complex with mitochondrial proteins.<sup>46</sup> Figure 2F further suggest that microparticle-bound CL, not CL micelles, is the predominant form in the circulation of TBI mice and that it promotes a hypercoagulable state in these mice.

In summary, a significant number of mitochondria are released into systemic circulation from traumatically injured brains during acute TBI. These mtMPs are highly procoagulant through the surface exposed CL. This novel mitochondrial procoagulant activity contributes to the hypercoagulable state that develops during acute TBI. The findings of this study as well as our recent report<sup>12</sup> suggest that cellular microparticles released from injured brains induce changes in coagulation that are detectable by laboratory measurements. These changes may be associated with the clinical coagulopathy in patients with TBI. This study can help identify new biomarkers and therapeutic targets for predicting and treating TBI-associated coagulopathy. The findings may also provide new sights into coagulation changes associated with injuries to other mitochondria-rich tissues and organs. Finally, the study offers new insights into the development of anti-CL antibody and the associated thrombotic phenotypes found in patients with antiphospholipid syndrome.

## References

- Hulka F, Mullins RJ, Frank EH. Blunt brain injury activates the coagulation process. *Arch Surg*. 1996;131(9):923-927.
- Hoots WK. Experience with antithrombin concentrates in neurotrauma patients. *Semin Thromb Hemost*. 1997;23(Suppl 1):3-16.
- Cap AP, Spinella PC. Severity of head injury is associated with increased risk of coagulopathy in combat casualties. *J Trauma*. 2011;71(1 Suppl):S78-S81.
- Sun Y, Wang J, Wu X, et al. Validating the incidence of coagulopathy and disseminated intravascular coagulation in patients with traumatic brain injury—analysis of 242 cases. *Br J Neurosurg*. 2011;25(3):363-368.
- Talving P, Benfield R, Hadjizacharia P, Inaba K, Chan LS, Demetriades D. Coagulopathy in severe traumatic brain injury: a prospective study. *J Trauma*. 2009;66(1):55-61.
- Stein SC, Young GS, Talucci RC, Greenbaum BH, Ross SE. Delayed brain injury after head trauma: significance of coagulopathy. *Neurosurgery*. 1992;30(2):160-165.
- Kaufman HH, Moake JL, Olson JD, et al. Delayed and recurrent intracranial hematomas related to disseminated intravascular clotting and fibrinolysis in head injury. *Neurosurgery*. 1980;7(5):445-449.
- Wafaisade A, Lefering R, Tjardes T, et al; Trauma Registry of DGU. Acute coagulopathy in isolated blunt traumatic brain injury. *Neurocrit Care*. 2010;12(2):211-219.
- Harhangi BS, Kompanje EJ, Leebeek FW, Maas AI. Coagulation disorders after traumatic brain injury. *Acta Neurochir (Wien)*. 2008;150(2):165-175.
- Salehpour F, Bazzazi AM, Porhomayon J, Nader ND. Correlation between coagulopathy and outcome in severe head trauma in neurointensive care and trauma units. *J Crit Care*. 2011;26(4):352-356.
- van der Sande JJ, Emeis JJ, Lindeman J. Intravascular coagulation: a common phenomenon in minor experimental head injury. *J Neurosurg*. 1981;54(1):21-25.
- Tian Y, Salsbery B, Wang M, et al. Brain-derived microparticles induce systemic coagulation in a murine model of traumatic brain injury. *Blood*. 2015;125(13):2151-2159.
- Zhang J, Jiang R, Liu L, et al. Traumatic brain injury-associated coagulopathy. *J Neurotrauma*. 2012;29(17):2597-2605.
- Exner T, Joseph J, Low J, Connor D, Ma D. A new activated factor X-based clotting method with improved specificity for procoagulant phospholipid. *Blood Coagul Fibrinolysis*. 2003;14(8):773-779.
- Tchaikovski SN, VAN Vlijmen BJ, Rosing J, Tans G. Development of a calibrated automated thrombography based thrombin generation test in mouse plasma. *J Thromb Haemost*. 2007;5(10):2079-2086.
- Poot M, Zhang YZ, Krämer JA, et al. Analysis of mitochondrial morphology and function with novel fixable fluorescent stains. *J Histochem Cytochem*. 1996;44(12):1363-1372.
- Mileykovskaya E, Dowhan W, Birke RL, Zheng D, Lutterodt L, Haines TH. Cardiolipin binds nonyl acridine orange by aggregating the dye at exposed hydrophobic domains on bilayer surfaces. *FEBS Lett*. 2001;507(2):187-190.
- Boudreau LH, Duchez AC, Cloutier N, et al. Platelets release mitochondria serving as substrate for bactericidal group IIA-secreted phospholipase A2 to promote inflammation. *Blood*. 2014;124(14):2173-2183.
- Lecocq J, Ballou CE. On the structure of cardiolipin. *Biochemistry*. 1964;3:976-980.
- Hovius R, Lambrechts H, Nicolay K, de Kruijff B. Improved methods to isolate and subfractionate rat liver mitochondria. Lipid composition of the inner and outer membrane. *Biochim Biophys Acta*. 1990;1021(2):217-226.
- de Kroon AI, Dolis D, Mayer A, Lill R, de Kruijff B. Phospholipid composition of highly purified mitochondrial outer membranes of rat liver and *Neurospora crassa*. Is cardiolipin present in the

## Acknowledgments

This study is supported by National Institutes of Health, National Institute of Neurological Disorders and Stroke grant NS087296, National Heart, Lung, and Blood Institute grant HL71895, and a bridge fund from American Society of Hematology (J.-f.D.); National Natural Science Foundation of China State Key Program grant 81330029, and National Natural Science Foundation of China research grants 81271361, 81271359 (J.Z.), and 81372575 (M.L.).

## Authorship

Contribution: Z.Z., M.W., Y.T., T.H., B.S., and E.B. performed experiments, analyzed data, and wrote the manuscript; E.Z.Z. performed experiments; X.W. developed new assays, analyzed data, and wrote the manuscript; P.T. provided key reagents and wrote the manuscript; M.L. formulated hypotheses, designed the study, analyzed data, and wrote the manuscript; J.Z. formulated hypotheses, designed the study, analyzed data, and wrote the manuscript; and J.-f.D. formulated hypotheses, designed the study, analyzed data, and wrote the manuscript.

Conflict-of-interest disclosure: The authors declare no competing financial interests.

Correspondence: Jing-fei Dong, BloodWorks Research Institute, 1551 Eastlake Ave East, Seattle, WA 98102; e-mail: jfdong@bloodworksnw.org; Jianning Zhang, Tianjin Neurological Institute, Department of Neurosurgery, Tianjin Medical University General Hospital, Tianjin 300052, China; e-mail: jianningzhang@hotmail.com; and Min Li, Institute of Pathology, School of Basic Medical Sciences, Lanzhou University, Lanzhou 730000, China; e-mail: limin@lzu.edu.cn.

- mitochondrial outer membrane? *Biochim Biophys Acta*. 1997;1325(1):108-116.
22. Hostetler KY, Zenner BD, Morris HP. Phosphatidylserine biosynthesis in mitochondria from the Morris 7777 hepatoma. *J Lipid Res*. 1979;20(5):607-613.
  23. Hostetler KY, Zenner BD, Morris HP. Phospholipid content of mitochondrial and microsomal membranes from Morris hepatomas of varying growth rates. *Cancer Res*. 1979;39(8):2978-2983.
  24. Vance JE, Tasseva G. Formation and function of phosphatidylserine and phosphatidylethanolamine in mammalian cells. *Biochim Biophys Acta*. 2013;1831(3):543-554.
  25. Shiao YJ, Lupo G, Vance JE. Evidence that phosphatidylserine is imported into mitochondria via a mitochondria-associated membrane and that the majority of mitochondrial phosphatidylethanolamine is derived from decarboxylation of phosphatidylserine. *J Biol Chem*. 1995;270(19):11190-11198.
  26. Achleitner G, Gaigg B, Krasser A, et al. Association between the endoplasmic reticulum and mitochondria of yeast facilitates interorganelle transport of phospholipids through membrane contact. *Eur J Biochem*. 1999;264(2):545-553.
  27. Dasgupta SK, Abdel-Monem H, Niravath P, et al. Lactadherin and clearance of platelet-derived microvesicles. *Blood*. 2009;113(6):1332-1339.
  28. Bayir H, Tyurin VA, Tyurina YY, et al. Selective early cardiolipin peroxidation after traumatic brain injury: an oxidative lipidomics analysis. *Ann Neurol*. 2007;62(2):154-169.
  29. Ji J, Kline AE, Amoscato A, et al. Lipidomics identifies cardiolipin oxidation as a mitochondrial target for redox therapy of brain injury. *Nat Neurosci*. 2012;15(10):1407-1413.
  30. Bornstein NM, Aronovich B, Korczy AD, Shavit S, Michaelson DM, Chapman J. Antibodies to brain antigens following stroke. *Neurology*. 2001;56(4):529-530.
  31. López-Escribano H, Miñambres E, Labrador M, Bartolomé MJ, López-Hoyos M. Induction of cell death by sera from patients with acute brain injury as a mechanism of production of autoantibodies. *Arthritis Rheum*. 2002;46(12):3290-3300.
  32. Ravanat C, Archipoff G, Beretz A, Freund G, Cazenave JP, Freyssinet JM. Use of annexin-V to demonstrate the role of phosphatidylserine exposure in the maintenance of haemostatic balance by endothelial cells. *Biochem J*. 1992;282(Pt 1):7-13.
  33. London F, Ahmad SS, Walsh PN. Annexin V inhibition of factor IXa-catalyzed factor X activation on human platelets and on negatively-charged phospholipid vesicles. *Biochemistry*. 1996;35(51):16886-16897.
  34. Boilard E, Duchez AC, Brisson A. The diversity of platelet microparticles. *Curr Opin Hematol*. 2015;22(5):437-444.
  35. Alberts B, Bray D, Lewis J, et al. *Intracellular Compartments and Protein Sorting*. Molecular Biology of the Cell. New York: Garland Publishing Inc.; 1994:551-598.
  36. Hiebert JB, Shen Q, Thimmesch AR, Pierce JD. Traumatic brain injury and mitochondrial dysfunction. *Am J Med Sci*. 2015;350(2):132-138.
  37. Itagaki K, Kaczmarek E, Lee YT, et al. Mitochondrial DNA released by trauma induces neutrophil extracellular traps. *PLoS One*. 2015;10(3):e0120549.
  38. Zhang Q, Raoof M, Chen Y, et al. Circulating mitochondrial DAMPs cause inflammatory responses to injury. *Nature*. 2010;464(7285):104-107.
  39. Cairns CB, Moore FA, Haenel JB, et al. Evidence for early supply independent mitochondrial dysfunction in patients developing multiple organ failure after trauma. *J Trauma*. 1997;42(3):532-536.
  40. Simmons JD, Lee YL, Mulekar S, et al. Elevated levels of plasma mitochondrial DNA DAMPs are linked to clinical outcome in severely injured human subjects. *Ann Surg*. 2013;258(4):591-596.
  41. Meers P, Mealy T. Calcium-dependent annexin V binding to phospholipids: stoichiometry, specificity, and the role of negative charge. *Biochemistry*. 1993;32(43):11711-11721.
  42. Andree HA, Reutelingsperger CP, Hauptmann R, Hemker HC, Hermens WT, Willems GM. Binding of vascular anticoagulant alpha (VAC alpha) to planar phospholipid bilayers. *J Biol Chem*. 1990;265(9):4923-4928.
  43. Tait JF, Gibson D. Phospholipid binding of annexin V: effects of calcium and membrane phosphatidylserine content. *Arch Biochem Biophys*. 1992;298(1):187-191.
  44. Chu CT, Ji J, Dagda RK, et al. Cardiolipin externalization to the outer mitochondrial membrane acts as an elimination signal for mitophagy in neuronal cells. *Nat Cell Biol*. 2013;15(10):1197-1205.
  45. Li N, Ragheb K, Lawler G, et al. Mitochondrial complex I inhibitor rotenone induces apoptosis through enhancing mitochondrial reactive oxygen species production. *J Biol Chem*. 2003;278(10):8516-8525.
  46. Rossen RD, Michael LH, Hawkins HK, et al. Cardiolipin-protein complexes and initiation of complement activation after coronary artery occlusion. *Circ Res*. 1994;75(3):546-555.
  47. Junker M, Creutz CE. Ca(2+)-dependent binding of endonexin (annexin IV) to membranes: analysis of the effects of membrane lipid composition and development of a predictive model for the binding interaction. *Biochemistry*. 1994;33(30):8930-8940.